



**HAL**  
open science

## 3D-Hopkinson Bar: New Experiments for Dynamic Testing on Soils

Jean-François Semblat, Minh-Phong Luong, Gérard Gary

► **To cite this version:**

Jean-François Semblat, Minh-Phong Luong, Gérard Gary. 3D-Hopkinson Bar: New Experiments for Dynamic Testing on Soils. *Soils and Foundations*, 1999, 39 (1), pp.1-10. 10.3208/sandf.39.1 . hal-04667429

**HAL Id: hal-04667429**

**<https://hal.science/hal-04667429v1>**

Submitted on 5 Aug 2024

**HAL** is a multi-disciplinary open access archive for the deposit and dissemination of scientific research documents, whether they are published or not. The documents may come from teaching and research institutions in France or abroad, or from public or private research centers.

L'archive ouverte pluridisciplinaire **HAL**, est destinée au dépôt et à la diffusion de documents scientifiques de niveau recherche, publiés ou non, émanant des établissements d'enseignement et de recherche français ou étrangers, des laboratoires publics ou privés.



Distributed under a Creative Commons Attribution - NonCommercial 4.0 International License

# 3D-HOPKINSON BAR: NEW EXPERIMENTS FOR DYNAMIC TESTING ON SOILS

JEAN-FRANÇOIS SEMBLAT<sup>i)</sup>, MINH PHONG LUONG<sup>ii)</sup> and GERARD GARY<sup>iii)</sup>

## ABSTRACT

The Split Hopkinson Pressure Bar method (S.H.P.B) provides a ready means for direct analysis of material dynamic response. Soil specimens generally present poor mechanical properties, thus the classical experimental device has to be adapted. An original experimental arrangement “*Three-Dimensional Split Hopkinson Pressure Bar*” (3D-SHPB) is proposed. It allows measurement of the complete three-dimensional dynamic response of soils. Experiments are oedometric type tests (rigid confining cylinder) involving dynamic radial stress measurement. Pseudo Poisson’s ratio is then determined and the influence of strain rate is shown. In addition, other types of confining systems are used: soft and semi-rigid confinement and low impedance tests are performed. Results on different loading paths are compared with others on sands and clays. Analysis at grain-size level gives further elements on the comminution process.

**Key words:** dynamic response, fracture energy, granular material, Hopkinson bar, pseudo Poisson’s ratio, soil dynamics, stress path (IGC: D7/E8)

## FAST LOADINGS ON SOILS

### *Introduction*

In soil dynamics, many different methods and problems are considered. However, there is no real unified approach to investigating similarly as various problems such as earthquake engineering, pile driving, dynamic compaction, vibratory isolation, etc. These diverse problems involve various frequency ranges or strain magnitudes. A tentative classification is proposed in Fig. 1, comparing different practical problems and tests in terms of frequency, strain magnitude and ratio between wave length and dimensions of the domain (or the specimen). For small values of this ratio  $\lambda/l_{ref}$ , wave propagation phenomena prevail (Fig. 1). Otherwise, they may be neglected and the «dynamic» material behaviour can be directly analysed. We considered two approaches: direct analysis of dynamic response of soils (Semblat, 1995a, b) and study of wave propagation phenomena in soils (Semblat, 1995a, 1997, 1998). This paper focuses on experimental studies dealing with dynamic soil response: first experiments in the 60’s, Hopkinson bar based methods in the 70’s and 80’s and our 3D-Split Hopkinson Pressure Bar (3D-SHPB), (Semblat, 1995a, b).

### *Previous Dynamic Experiments*

W. Heierli (1962) and R. V. Whitman (1957) investi-

gated dynamic soil response in the 60’s. However, they did not really take into account wave propagation phenomena in the experimental device itself. In the 70’s in France, G. Aussedat and J. Meunier (1974) developed dynamic tests on soils (falling mass with fast-speed imaging of the crushing phase). They also performed experiments based on the Split Hopkinson Pressure Bar method. They designed a low impedance bar (nylon) because their first experiments on steel bars were very disappointing.

Their work is among the first investigations of dynamic response of soils with an accurate control of transient phenomena in the experimental device itself. Split Hopkinson Pressure Bar tests (SHPB) seem to be well-adapted for soils and provide a good control of wave propagation phenomena.

## THE “TRADITIONAL” S.H.P.B METHOD

### *Experimental Arrangement*

The original Hopkinson device (with only one cylindrical bar) was modified by Kolsky (two bars) for indirect measurements on both sides of the specimen. The “traditional” Split Hopkinson Pressure Bar system is then composed of two axial bars (incident bar and transmitter bar) and a striker bar launched by a gas gun. Figure 2 schematically presents such a “traditional” SHPB device.

<sup>i)</sup> Research Engineer, Laboratoire Central des Ponts et Chaussées, Engineering Modeling Department, 58 bd Lefèbvre, 75732 Paris Cedex 15, France. (Semblat@lpc.fr)

<sup>ii)</sup> Research Director, National Center for Scientific Research (CNRS), Solid Mechanics Laboratory, Ecole Polytechnique, 91128 Palaiseau Cedex, France.

<sup>iii)</sup> Research Engineer, ditto.

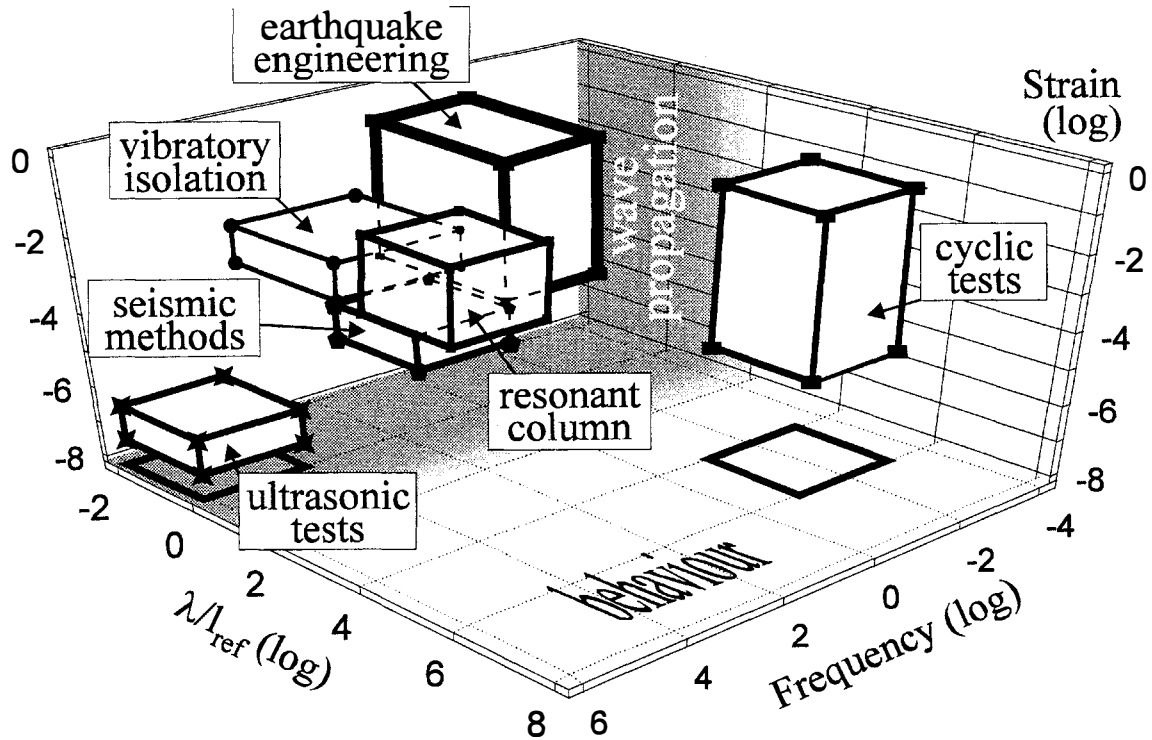


Fig. 1. Classification of dynamic tests on soils

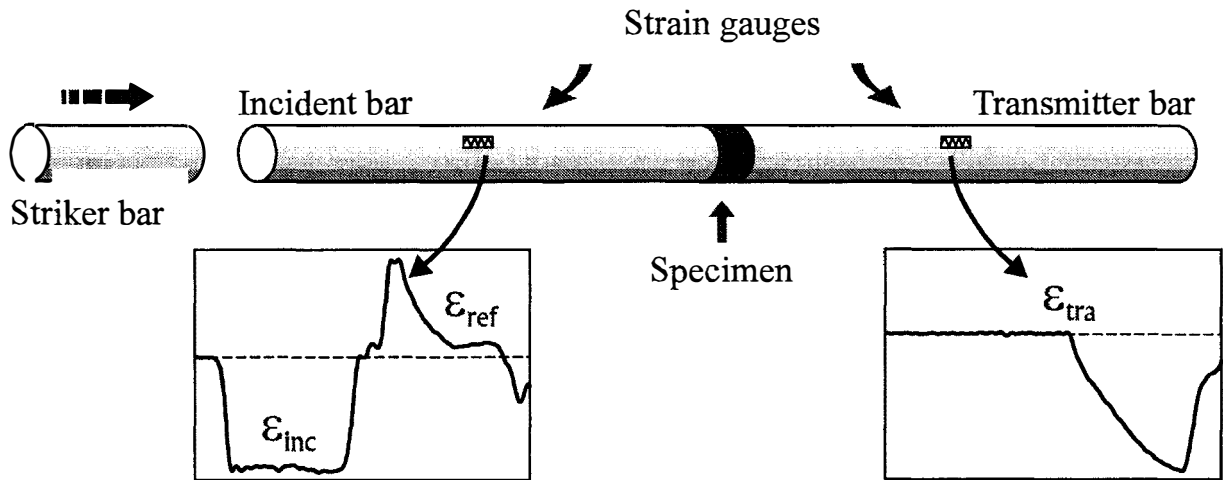


Fig. 2. "Traditional" Split Hopkinson Pressure Bar device

As shown in Fig. 2, the specimen is placed between two main bars. The main aim of Hopkinson type experiments is to perform indirect strain measurements: strains are measured on the bars (and not directly on the specimen). These measurements provide values of forces and displacements (stress and strain) at every location on the bars and at every time, particularly at bar-specimen interfaces.

#### Axial Stress in the Specimen

Propagation of stress wave in bars and through both bar-specimen interfaces is an important aspect of dynamic experiments on the S.H.P.B device. On both bar-speci-

men interfaces, a process of multiple reflections and transmissions takes place. A 3D-schematic is given by Semblat (1995a, b) depicting the variations of axial stress with time and location. It indicates clearly that axial stress in the specimen increases progressively. This stage of the experiment is called the "transient stage" during which propagation phenomena strongly prevail. Afterwards axial stress becomes more and more uniform along the specimen. This is the main interest of SHPB method: it allows *uniform stress distribution under high strain rates*.

#### Two Main Experimental Stages

As depicted in Fig. 3, dynamic tests on the Split Hop-

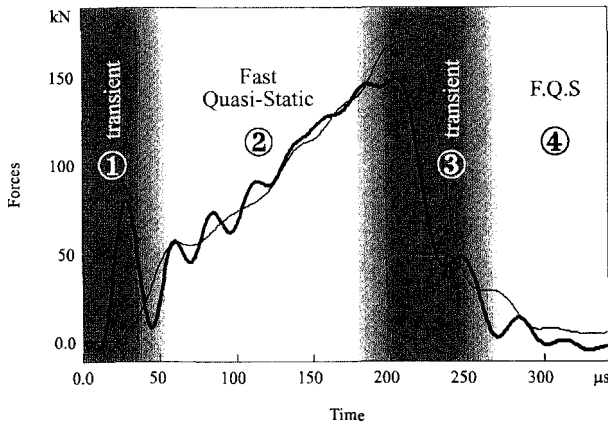


Fig. 3. Forces on both specimen sides showing two main stages of the SHPB experiment

kinson Pressure Bar can generally be divided in two main stages:

- a “transient stage”: the stress state is non homogeneous, wave propagation phenomena in the specimen strongly prevail
- a “fast quasi-static stage”: a stress equilibrium state along the specimen length is reached, the axial stress is homogeneous in the whole specimen (incident and transmitted forces are balanced).

From experimental results (Semblat, 1995a, b), it is obvious that both incident and transmitted forces are equal after the initial transient phase. As shown by Fig. 3, the classical assumption of the S.H.P.B method is fulfilled: it is possible to perform high strain rate experiments on soils since there is a “Fast Quasi-Static” stage allowing direct determination of the dynamic response (behaviour) of this soil. However, recent analysis techniques give much more information about transient stages (Rota, 1994).

#### Determination of Mechanical Parameters

As is shown in Fig. 2, strain waves are measured on the bars: incident and reflected waves on the incident bar and transmitted wave on the transmitter bar. However, to determine forces and displacements at both bar-specimen interfaces, strain waves have to be fictitiously carried to the interfaces. The most important thing is to identify the starting point of each strain wave. Elastic simulation of strain wave propagation in the specimen (Gary, 1992) allows, for example, a more precise identification (dispersive phenomena in the bars being also taken into account).

In the bars, behaviour and propagation parameters are readily related. Strain rate  $\dot{\epsilon}_{ax}(t)$  and axial stress  $\sigma_{ax}(t)$  are then given as follows:

$$\dot{\epsilon}_{ax}(t) = \frac{C_0}{h} \cdot [\epsilon_{tra}(t) + \epsilon_{ref}(t) - \epsilon_{inc}(t)] \quad (1)$$

$$\sigma_{ax}(t) = \frac{S_b E}{2S_{spec}} \cdot [\epsilon_{inc}(t) + \epsilon_{ref}(t) + \epsilon_{tra}(t)] \quad (2)$$

where  $C_0$  is the wave velocity in the bars,  $h$  the length of the specimen,  $S_{spec}$  its section area and  $\epsilon_{inc}$ ,  $\epsilon_{ref}$  and  $\epsilon_{tra}$  are the incident, reflected and transmitted strains respectively.

Since dispersive phenomena are corrected (Gary, 1992), the assumption of one-dimensional propagation is fully justified. Equation (2) is valid if axial forces on both sides of the specimen are equal. This is verified considering experimental results given in Fig. 3.

#### RECENT DYNAMIC EXPERIMENTS

A lot of recent research has provided results from Hopkinson type experiments on soils. C. W. Felice (1987, 1991) and G. E. Veyera (1995) in the USA, S. Shibusawa in Japan (1992) and A. M. Bragov (1994) in Russia performed SHPB tests to determine soil response under high strain rate.

C. W. Felice (1987, 1991) performed Hopkinson bar experiments on saturated sand (or clayey sand) specimens. These were oedometric dynamic tests (rigid confining cylinder) without measurements of radial stress. The main goal of this work was to improve the analysis of experimental results in the initial loading phase. Slenderness of the specimens was less than 0.2 for a bar diameter of  $\Phi = 60.3$  mm (see Table 1). Experimental results indicated that specimen resistance increases because of saturation. Veyera and Ross (1995) works concerned sand specimens under undrained dynamic compression using a thick-walled container. Specimens length ranged from  $l = 6.3$  to  $l = 12.7$  mm and the bar diameter was  $\Phi = 50.8$  mm. The strain rates involved in these experiments were from 1000 to 2000  $s^{-1}$  (see Table 1).

In Japan, Shibusawa and Oida (1992) investigated the dynamic response of soils (mainly clays) to study the influence of water content and specimen dimensions. The experimental device allows measurement of incident and reflected waves only. The transmitted force is measured directly on the specimen (see Table 1). Shibusawa and Oida gave prominence to an exponential increase of the dynamic modulus with increasing water content.

A. M. Bragov (1994) studied the dynamic response of plasticine in jacket-confined tests. The bars diameter was  $\Phi = 20$  mm and the specimen length was  $l = 15$  mm. This was with our work, the first research to investigate three-dimensional dynamic response by performing circumferential strain measurement. Bragov uses four strain gauges on the jacket to determine the radial strain of the specimen during dynamic axial loading (see Table 1).

The main characteristics of the tests performed by these different authors are collected in Table 1. Experimental devices were all Hopkinson type systems (with only one bar for Shibusawa (1992)). The dimensions of bars, specimens and the confining methods used varied: confining cylinder, confining pressure (see Table 1). The results of our approach will be compared with those obtained by the authors listed in Table 1.

**Table 1. Different Hopkinson type dynamic tests on soils**

Authors	Type of soil	Specimen size	Striker & bars	Duration	Confinement
Meunier (1974)	clay	$l=2 \text{ \AA } 15 \text{ mm}$ $\phi=36 \text{ mm}$	$l_{\text{stri}}=0.15 \text{ m}$ nylon $\phi=36 \text{ mm}$	$500 \mu\text{s}$	air pressure
Felice (1987, 1991)	clayey sand and alluv.	$l=13/25 \text{ mm}$ $\phi=60.9 \text{ mm}$	$l_{\text{stri}}=0.25 \text{ m}$ metal $\phi=60.9 \text{ mm}$	$125 \mu\text{s}$	thick cylinder
Bragov (1994)	plasticine ( $\Rightarrow$ clay)	$l=15 \text{ mm}$ $\phi=20 \text{ mm}$	$l_{\text{stri}}=0.25 \text{ m}$ metal $\phi=20 \text{ mm}$	$200 \mu\text{s}$	thin cylinder th. = 10 mm measur. of $\epsilon_r$
Veyera (1995)	dry or saturated sand	$l=6.3/12.7 \text{ mm}$ $\phi=50.8 \text{ mm}$	$l_{\text{stri}}=0.65 \text{ m}$ metal $\phi=50.8 \text{ mm}$	$257 \mu\text{s}$	thick cylinder: th. = 25 mm
Shibusawa (1992)	silt + clay + sand	$l=50/100 \text{ mm}$ $\phi=50 \text{ mm}$	$l_{\text{stri}}=0.25 \text{ m}$ metal $\phi=25 \text{ mm}$	$80 \mu\text{s}$	none
Semlat, Luong, Gary (1995a, b)	dry sand	$l=10, 15, 20, 25$ & $30 \text{ mm}$ $\phi=40 \text{ mm}$	$l_{\text{stri}}=0.85 \text{ m}$ & $0.5 \text{ m}$ metal & PMMA $\phi=40 \text{ mm}$	$350 \mu\text{s}$	thick cylinder air pressure oil pressure

### “3D-SHPB”: A NEW DEVICE FOR DYNAMIC TESTING ON SOILS

For the dynamic testing of soils, it is necessary to modify the classical Hopkinson arrangement: Meunier proposed a nylon bars device, Felice used a rigid confining cylinder, and Bragov confined experiments (Table 1). However, considering the influence of stress path on soils response, it would be very interesting to measure (or control) both axial and radial stresses. In this study, oedometric dynamic tests using a rigid confining cylinder are carried out on a special device called “*Three-Dimensional Split Hopkinson Pressure Bar*” (3D-SHPB). When using a rigid confining cylinder, zero radial strain can be ensured while radial stress cannot be correctly estimated. Using a radial bar in contact with the specimen

through the confining cylinder, this special device allows measurement of radial stress with time (Semlat, 1995a, b). Figure 4 gives a schematic view of the “*Three-Dimensional Split Hopkinson Pressure Bar*”.

The special device involves three Hopkinson type bars: 2 axial bars to measure axial displacements and forces on both sides of the specimen, and 1 radial bar to evaluate the radial stress during the test. Mechanical and geometrical characteristics of the axial bars are given in Table 2.

### RIGID CONFINEMENT TESTS (DYNAMIC OEDOMETRIC)

#### *Axial Dynamic Response*

All the specimens are composed of dry Fontainebleau sand. Density of the specimens is constant:  $\rho=1667 \text{ kg/}$

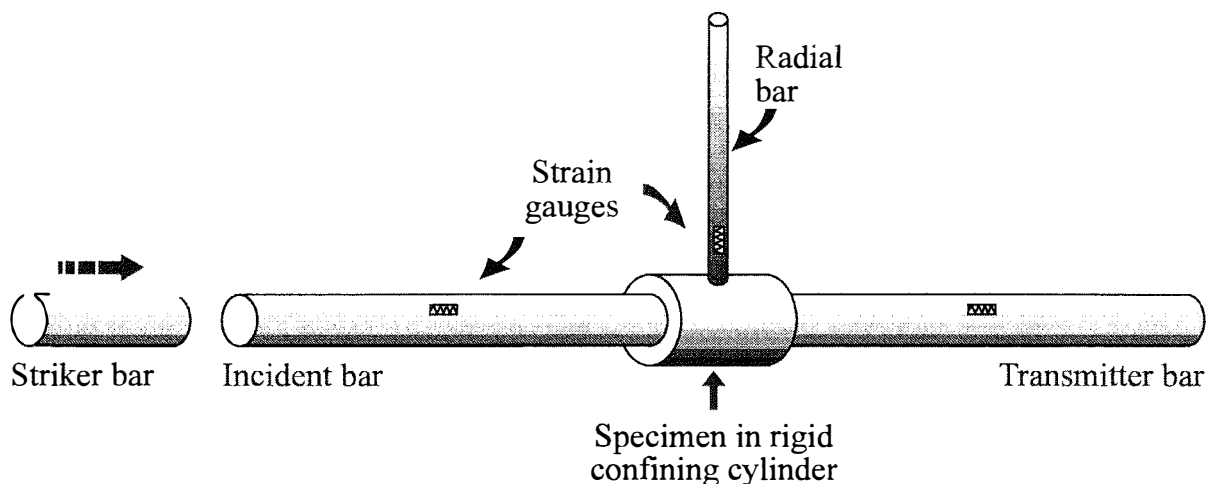


**Fig. 4. Three-Dimensional Split Hopkinson Pressure Bar device**

Table 2. Bar and striker bar characteristics

Bar characteristics		Striker characteristics	
diameter	$\Phi=40$ mm	diameter	$\Phi=40$ mm
length	$l_b=2$ m	length	$l_s=0.85$ m
Young modulus	$E=70000$ MPa	Young modulus	$E=70000$ MPa
density	$\rho_b=2820$ kg/m <sup>3</sup>	mass	$m=3.012$ kg
velocity	$C_0=5180$ m/s	impact speed	2 to 20 m/s

m<sup>3</sup>. The tests performed on the experimental device shown in Fig. 4 are called ‘‘rigid confinement tests’’: the rigid confining cylinder prevents radial strain. The confining cylinder must therefore be sufficiently rigid or thick to give a small radial strain. This is verified from radial stress measurements and numerical results given in Semblat (1995b). For rigid confinement tests (Fig. 5), axial responses are nearly linear for loading and unloading phases with different slopes in both cases but equivalent ones from one test to another. The elastic part of the response is not really clear as the global dynamic behaviour of sand is shown to be highly anelastic. The oedometric response is compared further with responses on other kind of loading paths.

#### Dynamic Moduli of Sand

The oedometric dynamic tests are performed using specimens of five different lengths and three impact speeds (of the striker bar on the incident bar), each test being repeated three times identically. For all these tests, values of corresponding strain rates and dynamic moduli are given in Table 3. Strain rate values range from 200 s<sup>-1</sup> up to 1245 s<sup>-1</sup> depending on the impact speed (of the striker bar on the incident bar) and on the specimen length. Slopes of the dynamic stress-strain curves refer to a highly anelastic, but linear, dynamic response and range from 350 MPa to 750 MPa approximately (*see* Table 3).

From the experimental results, it is clear that variations of these slopes are not negligible at all, but the relationship with strain rate values is not obvious. Analysis of three-dimensional aspects of the dynamic response gives interesting results concerning the potential dynamic effect.

#### Radial Stress Measurement

The confining pressure is not constant during axial dynamic loading. To quantify the variations of radial stress with time, an original experimental arrangement is proposed. The 3D-SHPB device (Fig. 4) allows the measurement of the stress wave in the radial bar from which the radial stress in the specimen is derived. It is then possible to compare values of axial and radial stress with time (Semblat, 1995a, b). Mechanical and geometrical properties of the radial bar are given in Table 4.

#### Test Reproducibility

Experimental reproducibility is studied by repeating

Table 3. Experimental results for all oedometric dynamic tests

Test	Spec. length	Impact speed	Strain rate	Modulus	Mean modul.
001			393 s <sup>-1</sup>	468 MPa	
002		3.4 m · s <sup>-1</sup>	473 s <sup>-1</sup>	479 MPa	476 MPa
003			497 s <sup>-1</sup>	482 MPa	
006			771 s <sup>-1</sup>	377 MPa	
007	10 mm	5.8 m · s <sup>-1</sup>	725 s <sup>-1</sup>	443 MPa	426 MPa
008			697 s <sup>-1</sup>	457 MPa	
011			1245 s <sup>-1</sup>	440 MPa	
012		9.9 m · s <sup>-1</sup>	1190 s <sup>-1</sup>	476 MPa	460 MPa
013			1188 s <sup>-1</sup>	464 MPa	
016			345 s <sup>-1</sup>	515 MPa	
017		3.4 m · s <sup>-1</sup>	314 s <sup>-1</sup>	502 MPa	509 MPa
018			279 s <sup>-1</sup>	511 MPa	
021			468 s <sup>-1</sup>	582 MPa	
022	15 mm	5.8 m · s <sup>-1</sup>	458 s <sup>-1</sup>	602 MPa	591 MPa
023			446 s <sup>-1</sup>	588 MPa	
026			793 s <sup>-1</sup>	593 MPa	
027		9.9 m · s <sup>-1</sup>	821 s <sup>-1</sup>	604 MPa	589 MPa
028			827 s <sup>-1</sup>	571 MPa	
031			220 s <sup>-1</sup>	648 MPa	
032		3.4 m · s <sup>-1</sup>	240 s <sup>-1</sup>	719 MPa	700 MPa
033			268 s <sup>-1</sup>	732 MPa	
036			379 s <sup>-1</sup>	557 MPa	
037	20 mm	5.8 m · s <sup>-1</sup>	361 s <sup>-1</sup>	582 MPa	570 MPa
038			359 s <sup>-1</sup>	570 MPa	
041			634 s <sup>-1</sup>	616 MPa	
042		9.9 m · s <sup>-1</sup>	640 s <sup>-1</sup>	619 MPa	626 MPa
043			602 s <sup>-1</sup>	644 MPa	
046			200 s <sup>-1</sup>	704 MPa	
047		3.4 m · s <sup>-1</sup>	222 s <sup>-1</sup>	679 MPa	693 MPa
048			223 s <sup>-1</sup>	695 MPa	
049			318 s <sup>-1</sup>	655 MPa	
050	25 mm	5.8 m · s <sup>-1</sup>	316 s <sup>-1</sup>	649 MPa	661 MPa
051			317 s <sup>-1</sup>	679 MPa	
052			508 s <sup>-1</sup>	657 MPa	
053		9.9 m · s <sup>-1</sup>	521 s <sup>-1</sup>	664 MPa	661 MPa
054			536 s <sup>-1</sup>	661 MPa	
055			167 s <sup>-1</sup>	686 MPa	
056		3.4 m · s <sup>-1</sup>	148 s <sup>-1</sup>	670 MPa	697 MPa
057			158 s <sup>-1</sup>	735 MPa	
058			264 s <sup>-1</sup>	684 MPa	
059	30 mm	5.8 m · s <sup>-1</sup>	270 s <sup>-1</sup>	684 MPa	700 MPa
060			247 s <sup>-1</sup>	733 MPa	
061			444 s <sup>-1</sup>	635 MPa	
062		9.9 m · s <sup>-1</sup>	430 s <sup>-1</sup>	692 MPa	657 MPa
063			455 s <sup>-1</sup>	645 MPa	

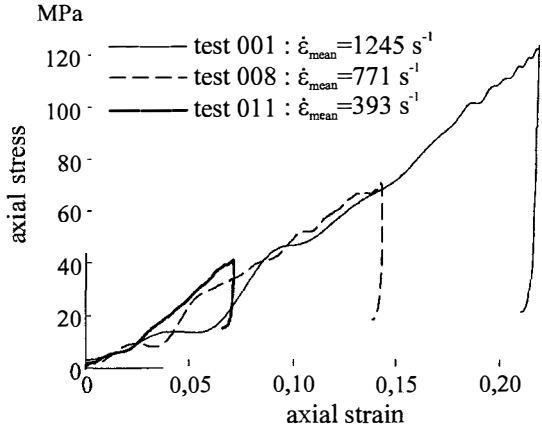


Fig. 5. Dynamic response on 3D-S.H.P.B

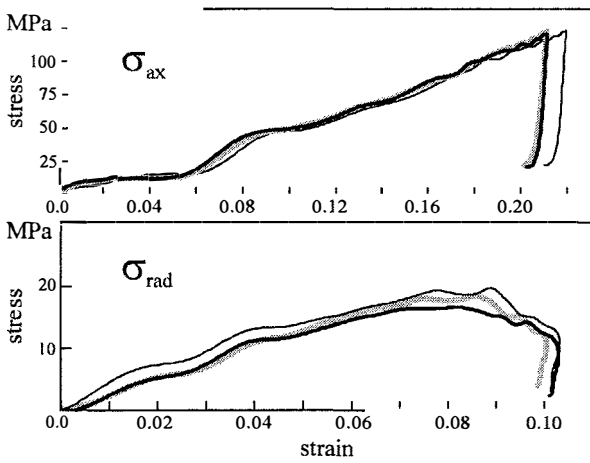


Fig. 6. Axial and radial stresses versus strain for three identical tests

Table 4. Radial bar characteristics

Radial bar	
diameter	$\phi = 40 \text{ mm}$
length	$l_b = 1.442 \text{ m}$
Young modulus	$E = 94000 \text{ MPa}$
density	$\rho_b = 8520 \text{ kg/m}^3$
velocity	$C_0 = 3323 \text{ m/s}$

each tests (specimen length, strain rate) three times identically. This is very good for axial stress, and acceptable for radial stress measurements (see Fig. 6 and Table 3).

### THREE-DIMENSIONAL ASPECTS OF DYNAMIC LOADING

#### Mean and Deviatoric Stresses

Starting from the axial and radial stress measurements, it is possible to evaluate the three-dimensional loading path in terms of mean stress “ $p$ ” and deviatoric stress “ $q$ ”. Figure 7 curves reveal clearly that, for a linear

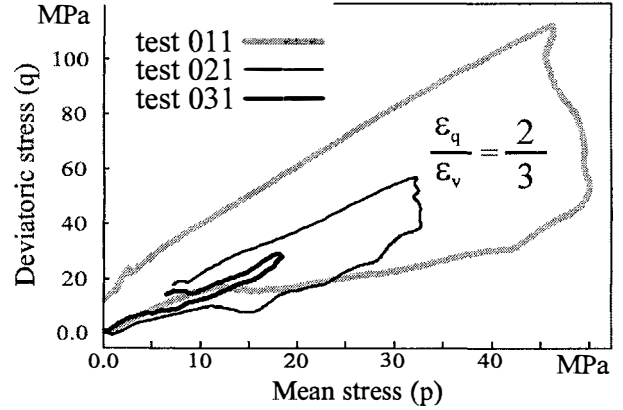


Fig. 7.  $p$ - $q$  diagrams: deviatoric stress versus mean stress (oedometric dynamic tests)

strain path ( $\varepsilon_q/\varepsilon_v=2/3$  in oedometric tests), the stress path is also linear. However, loading slope and unloading slope on  $p$ - $q$  diagrams are different. The structure of the specimen is actually different after the loading stage (grain crushing, see last section).

Comparisons of axial and radial stresses provide more quantitative results in the next paragraph. In the following section, other tests are performed under constant and slightly variable confining pressures. This allows the comparison of stress paths for various confining conditions under high strain rates.

#### Pseudo Poisson's Ratio

From measurements, it is possible to investigate further the three-dimensional dynamic response. Considering the oedometric strain paths used and the quasi-linear aspect of the axial dynamic response, a *dynamic pseudo Poisson's ratio* can be calculated using the theory of elasticity. Stress and strain tensors are then very simply related:

$$\varepsilon_{22} = \frac{\sigma_{22}}{E} - \frac{\nu}{E} (\sigma_{11} + \sigma_{33}) \quad \text{for example.}$$

For rigid confinement tests, we assume that principal stress and strain directions are the same as axial and radial bars directions. As these tests are oedometric,  $\varepsilon_{22}$  is zero,  $\sigma_{11} = \sigma_{ax}$  and  $\sigma_{22} = \sigma_{33} = \sigma_{rad}$  (where  $\sigma_{ax}$  and  $\sigma_{rad}$  are the axial and radial stresses respectively). The previous relationship gives the expression of the *dynamic pseudo Poisson's ratio*

$$\nu = \frac{\sigma_{rad}}{\sigma_{ax} + \sigma_{rad}} \quad (3)$$

From the experimental measurements of axial and radial stresses and the previous expression of dynamic pseudo Poisson's ratio  $\nu_{dyn}$  (Eq. 6), corresponding numerical values are derived. Curves of Fig. 8 give values of  $\nu_{dyn}$  for three identical tests (see Table 3). After the initial transient stage ( $\varepsilon < 0.015$ ), values of  $\nu_{dyn}$  have slight variations with axial strain. The dynamic pseudo Poisson's ratio is then really found to be a nearly constant parameter relating axial and radial stresses. Values of  $\nu_{dyn}$  given in Table

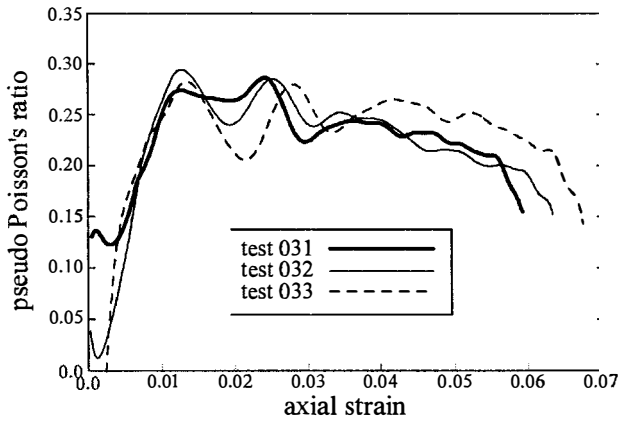


Fig. 8. Dynamic pseudo Poisson's ratio for three identical oedometric tests

Table 5. Dynamic pseudo Poisson's ratio for oedometric dynamic tests

Test/strain rate	$v_{dyn}$	Mean value
011/1245 s <sup>-1</sup>	0.33	
012/1190 s <sup>-1</sup>	0.39	0.37
013/1188 s <sup>-1</sup>	0.39	
021/468 s <sup>-1</sup>	0.32	
022/458 s <sup>-1</sup>	0.30	0.31
023/446 s <sup>-1</sup>	0.30	
031/220 s <sup>-1</sup>	0.24	
032/240 s <sup>-1</sup>	0.24	0.24
033/268 s <sup>-1</sup>	0.25	

5 correspond to various specimen lengths and strain rates. It appears from these values that the pseudo Poisson's ratio is the highest for highest values of strain rate (Table 3). The pseudo Poisson's ratio changes from one group of identical tests to another because the dynamic radial confining effect increases with increasing strain rate.

## OTHER LOADING PATHS

### Various Types of Confinement

In addition to the "rigid confinement" tests (oedometric tests on 3D-SHPB), three other types of confining systems are used: *semi-rigid confinement* (slightly variable confining pressure), *soft confinement* (constant confining pressure), *low impedance tests* (plexiglas bars with low mechanical impedance). "Low impedance" tests are performed on a PMMA Hopkinson device and the specimen is confined with a constant pressure (Semblat, 1995a, b). A special correction procedure allows us to take into account damping and dispersive phenomena in the viscoelastic bars used (Zhao, 1997).

### Semi-rigid Confinement Tests

Semi-rigid confinement tests are performed under slightly variable confinement. The experimental device does not allow an accurate estimation of confining pressure variations. Figure 9 gives the axial stress versus axial strain for different semi-rigid confinement tests (slightly variable confinement). For this kind of test, the dynamic response is nearly linear for both loading and unloading. Values of axial stress are of the same order as for rigid confinement tests. Curves presented in Fig. 9 refer to tests performed under various confining pressures (3.0; 5.6 and 7.5 MPa) but with the same specimen length ( $l=10$  mm). Confining pressure has no strong influence on the dynamic response (for the present confining pressure values). It should be noted that this pressure may change during axial loading (no measurement of these changes is performed here).

### Soft Confinement Tests

Soft confinement tests are performed under constant confining air pressure. Figure 9 gives the axial stress versus axial strain for a confining pressure of 2.5 MPa; the specimen length is  $l=11$  mm. The maximum value of axial stress is 40 MPa, which is much lower than values of rigid or semi-rigid confinement tests. For soft confinement tests, the response is no more linear for the loading phase. For rigid and semi-rigid confinement tests, the variations of confinement during loading give a stiffened response of the material.

### Low Impedance Tests (PMMA Bars)

Low impedance tests are performed on a PMMA bar (plexiglas). These bars have a much lower mechanical impedance than the duraluminium bars used for all other tests (see Table 6). The strain measurements made on the bars are corrected by taking into account both geometrical dispersion in the bars and material dispersion due to plexiglas viscosity (Zhao, 1997).

Figure 9 gives three curves: axial stress versus axial strain from low impedance tests. The maximum axial stress is much lower than for other types of tests (less than 10 MPa). The dynamic response of the material is of the softening type even if strain rates are of the same order as for the previous tests.

## COMPARISON OF THE DYNAMIC RESPONSES

### Influence of the Dynamic Loading Path

From the different dynamic tests performed, it is possible to appreciate the influence of stress path on the specimen response. Comparison of the dynamic responses on different loading paths (rigid confining, semi-rigid, soft and low impedance) is given in Fig. 9. From these curves, there is an obvious influence of the dynamic loading path on the dynamic response. There are two kinds of dynamic response:

- for "low impedance" and "soft confinement" tests (bottom curves in Fig. 9): the flexibility of the confinement cannot firmly control the volumetric strain and



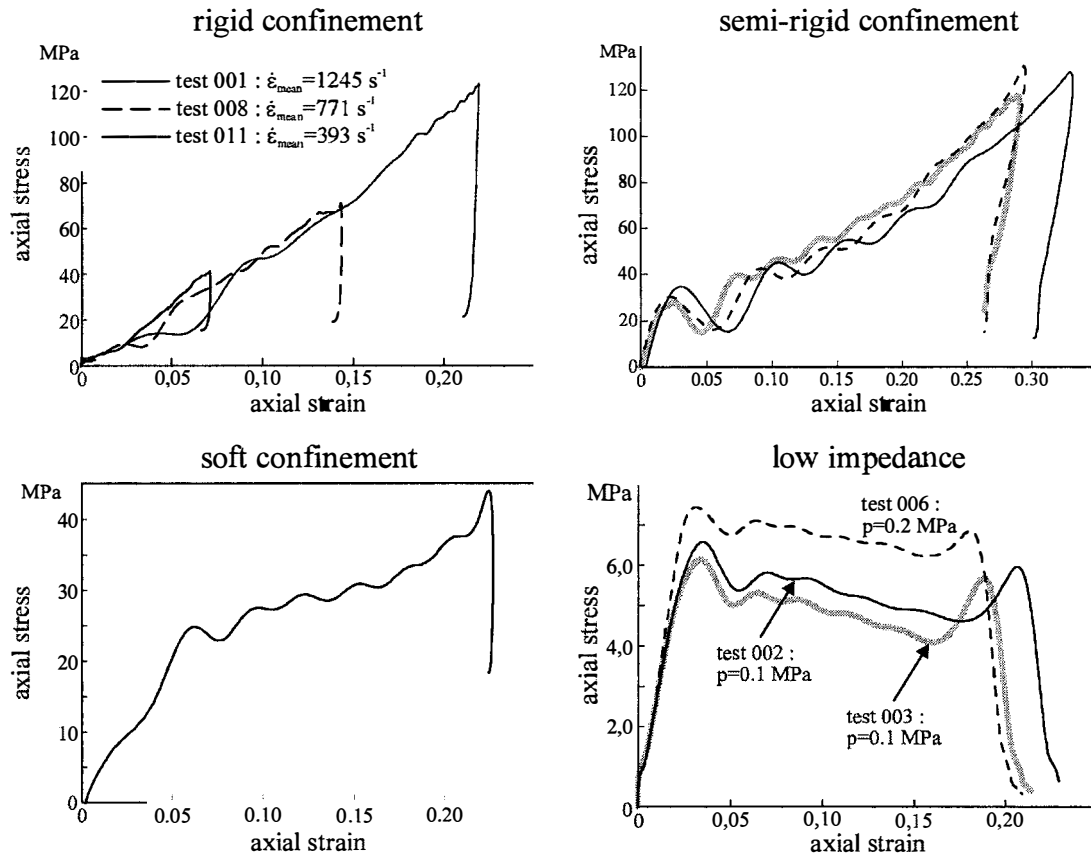


Fig. 9. Axial stress-strain curves for different types of confinement

Table 6. Bar characteristics for low impedance tests

Bar characteristics	
diameter	$\phi = 40$ mm
length	$l_b = 2$ m
Young modulus	$E = 6000$ MPa
density	$\rho_b = 1226$ kg/m <sup>3</sup>
velocity	$C_0 = 2210$ m/s

thus allows strain-softening of the specimen during dynamic loading,

- for “semi-rigid confinement” tests and “oedometric tests”: behaviour is quite linear for loading. The increase of the confinement apparently strengthens the specimen under dynamic loading.

#### Other Experimental Investigations

Other authors have studied soil response under fast loadings (Table 1). It started with Heierli and Whitman in the late 50's, but there was no appropriate control of the dynamic processes in the experimental device itself. Most recent investigations use Hopkinson type experimental arrangements (Table 8). Transient phenomena are well-controlled and a special confining procedure is generally used. The only work considering three-dimen-

Table 7. Mean grain diameter after different dynamic tests (rigid confinement)

Test	Strain rate	Mean diameter
virgin	—	196 $\mu\text{m}$
001	393 s <sup>-1</sup>	185 $\mu\text{m}$
006	771 s <sup>-1</sup>	151 $\mu\text{m}$
011	1245 s <sup>-1</sup>	66 $\mu\text{m}$
016	345 s <sup>-1</sup>	174 $\mu\text{m}$
021	468 s <sup>-1</sup>	137 $\mu\text{m}$
028	827 s <sup>-1</sup>	91 $\mu\text{m}$
031	220 s <sup>-1</sup>	176 $\mu\text{m}$
036	379 s <sup>-1</sup>	150 $\mu\text{m}$
041	634 s <sup>-1</sup>	104 $\mu\text{m}$
046	200 s <sup>-1</sup>	177 $\mu\text{m}$
049	318 s <sup>-1</sup>	172 $\mu\text{m}$
052	508 s <sup>-1</sup>	118 $\mu\text{m}$
055	167 s <sup>-1</sup>	182 $\mu\text{m}$
058	264 s <sup>-1</sup>	183 $\mu\text{m}$
061	444 s <sup>-1</sup>	121 $\mu\text{m}$

**Table 8. Main results for Hopkinson type dynamic tests given in Table 1**

Authors	Main results and conclusions
Meunier (1974)	<ul style="list-style-type: none"> <li>• first tests on nylon bars (low impedance) without correction of dispersive phenomena</li> <li>• weak influence of confining pressure on the response</li> </ul>
Felice (1987, 91)	<ul style="list-style-type: none"> <li>• bilinear behaviour:               <ul style="list-style-type: none"> <li>*1st phase for <math>\epsilon &lt;</math> initial porosity, filling of the voids and crushing of the grains</li> <li>*2nd phase specimen fully saturated, response of the fluid</li> </ul> </li> </ul>
Bragov (1994)	<ul style="list-style-type: none"> <li>• measurement of the circumferential strain from tests with soft confining cylinder on plasticine specimen</li> </ul>
Veyera (1995)	<ul style="list-style-type: none"> <li>• strong dependence of the dynamic response on the saturation index (stiffened behaviour with increasing saturation)</li> </ul>
Shibusawa (1992)	<ul style="list-style-type: none"> <li>• modulus increases with saturation</li> <li>• one-bar test, results deduced from incident and reflected waves only, axial stress possibly non homogeneous</li> </ul>
Semblat, Luong, Gary (1995a, b)	<ul style="list-style-type: none"> <li>• determination of the three-dimensional dynamic stress path, design of the <i>3D-S.H.P.B test</i></li> <li>• comparison of dynamic responses on different loading paths (rigid, semi-rigid, and soft confinements)</li> <li>• confinement increases stiffness of the dynamic response</li> <li>• evaluation of the dynamic pseudo Poisson's ratio</li> <li>• analysis at grain-size scale</li> </ul>

sional effects is due to Bragov, but he studied different loading paths than ours (his results concern *dynamic strain paths*). Our experiments give dynamic soil responses on various stress paths using the same material (see Table 8).

The influence of saturation on the dynamic response seems to be important after the initial phase of closing of the voids (Table 8). Our experiments do not investigate the influence of saturation but show the effect of confinement stiffness on the dynamic response (soft, semi-rigid and rigid). The influence of strain rate on the dynamic pseudo Poisson's ratio  $\nu_{\text{dyn}}$  is shown. Analysis at grain-size level is also an original aspect of our research and it could be related, in future works, with experiments made to study transient effects in granular forces variations (Semblat, 1995b).

## ANALYSIS AT GRAIN-SIZE LEVEL

### Grain-size Changes

For all the "rigid confinement" tests, grain-size distributions of the specimens are compared. As shown by Table 7, percentages of large grains decrease whereas percentages of small grains increase (Semblat, 1995a, b). As a result of this qualitative remark, it is possible to quantify the variations of particle size. The mean diameter for the virgin specimen is  $d_{\text{mean}} = 196 \mu\text{m}$ . After testing, the mean diameter may fall down to  $66 \mu\text{m}$ . The relationship

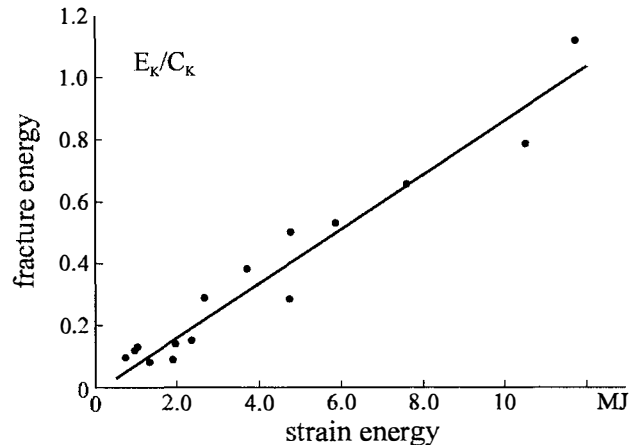


**Fig. 10. Fracture energy versus strain energy (for all oedometric tests)**

between grains mean diameter after testing and axial stress is strong. This may suggest out that there is no dynamical effect in the comminution phenomena.

### Fracture Energy

Considering variations of grains diameter, it is possible to make a quantitative analysis of the grains fracture in the specimen. Each grain-size curve may be related to the fracture energy of the corresponding test (Fukumoto, 1992). From (axial) stress-strain curves, *strain energy* dissipated in the specimen  $E_{\sigma-\epsilon}$  may also be estimated. As is shown in Fig. 9, for all oedometric dynamic tests, *fracture energy is proportional to strain energy*  $E_{\sigma-\epsilon}$ . Thus there is a close relationship between *strain energy* dissipated in the specimen (estimated from the response) and *fracture energy* (computed from theoretical expressions given in Semblat (1995a, b)). However, after loading of the specimen, some of the stress waves are still travelling in the bars. Nevertheless, from this relationship between fracture energy and strain energy, it seems that only the first loading wave changes grain-size distributions. This is a logical conclusion considering velocities at both bar-specimen interfaces after unloading (Semblat, 1995a). There is a separation between the bars and the specimen after the first unloading stage.

## CONCLUDING REMARKS

Using S.H.P.B loading to investigate the dynamic response of soil appears to be a promising approach. An original experimental arrangement is proposed to determine the whole 3D stress path (3D-Split Hopkinson Pressure Bar). The comparison of different tests using various confining conditions shows the strong influence of the loading path on the dynamic response. Calculation of dynamic pseudo Poisson's ratio reveals the strain rate effect on the 3D-dynamic response. Analysis at grain-size scale also gives interesting results about the relation between dynamic response and grain-size changes.

## ACKNOWLEDGEMENTS

The authors thank F. Darve Head of *GRECO-Géomatériaux* and J. P. Touret Coordinator of the Soil Dynamics Group for their friendly support to this research.

## REFERENCES

- 1) Bragov, A. M. (1994): "Use of the Kolsky method for studying shear resistance of soils," *DYMAT J.*, Vol. 1, No. 3, pp. 253-259.
- 2) Felice, C. W., Gaffney, E. S. and Brown, J. A. (1987): "Dynamic high stress experiments on soil," *Geotechnical Testing J.*, Vol. 10, No. 4, pp. 192-202.
- 3) Felice, C. W., Gaffney, E. S. and Brown, J. A. (1991): "Extended split Hopkinson bar analysis for attenuating materials," *J. of Engrg. Mechanics, ASCE*, Vol. 117, No. 5, pp. 1119-1135.
- 4) Fukumoto, T. (1992): "Particle breakage characteristics of granular soils," *Soils and Foundations*, Vol. 32, No. 1, pp. 26-40.
- 5) Gary, G., Klepaczko, J. R. and Zhao, H. (1992): "Corrections for wave dispersion and analysis of small strains with Split Hopkinson Bar," *Proc. of "Int. Symp. of Impact Engrg."*, Sendai, Japan.
- 6) Heierli, W. (1962): "Inelastic wave propagation in soil columns," *J. of the Soil Mechanics and Foundation Div., ASCE*, Vol. 88, No. SM6, pp. 33-63.
- 7) Meunier, J. (1974) "Contribution à l'étude des ondes et des ondes de choc dans les sols," PhD Thesis, Grenoble Univ.
- 8) Rota, L. (1994): "An inverse approach for identification of dynamic constitutive equations," *Proc. of 2nd Int. Symp. on Inverse Problems*, Bui, H. D. and Tanaka, M. (eds.), Paris.
- 9) Sadd, M. H., Qiu, L., Boardman, W. G. and Shukla, A. (1992): "Modelling wave propagation in granular media using elastic networks," *Int. J. of Rock Mechanics and Mining Science*, Vol. 29, No. 2, pp. 161-170.
- 10) Semblat, J. F. (1995a): "Soils under dynamic and transient loadings: dynamic response on Hopkinson bars, wave propagation in centrifuged medium" (in French), PhD Thesis (Ecole Polytechnique), "Etudes et Recherches des Laboratoires des Ponts et Chaussées," No. GT60, p. 206, Lab. Central des Ponts & Chaussées, Paris.
- 11) Semblat, J. F., Gary, G. and Luong, M. P. (1995b): "Dynamic response of sand using 3D-Hopkinson Bar," *Proc. of IS-Tokyo'95, 1st Int. Conf. on Earthquake Geotech. Engrg.*, Tokyo, 14-16 November, Balkema.
- 12) Semblat, J. F. (1997): "Rheological interpretation of rayleigh damping," *J. of Sound and Vibration*, Vol. 206, No. 5, pp. 741-744.
- 13) Semblat, J. F. and Luong, M. P. (1998): "Wave propagation through soils in centrifuge testing," *J. of Earthquake Engrg.*, Vol. 2, No. 1, pp. 147-171.
- 14) Shibusawa, S. and Oida, A. (1992): "Dependency of observation parameters on soil dynamic parameters in unconfined impact compression tests," *J. of Terramechanics*, Vol. 29, No. 3, pp. 289-306.
- 15) Veyera, G. E. and Ross, C. A. (1995): "High strain rate testing of unsaturated sands using a S.H.P.B.," *Proc. 3rd Int. Conf. on Recent Advances in Geotech. Earthquake Engrg. and Soil Dynamics*, pp. 31-34, St-Louis.
- 16) Whitman, R. V. (1957): "The behaviour of soils under transient loadings," *Proc. 4th Int. Conf. on SMFE*, Vol. 1, p. 207, London.
- 17) Zhao, H., Gary, G. and Klepaczko, J. R. (1997): "On the use of a viscoelastic Split Hopkinson Pressure Bar," *Int. J. of Impact Engrg.*, No. 19, pp. 319-330.